REPORT DOCUMENTATION PAGE

Form Approved OMB NO. 0704-0188

1. REPORT DATE (DD-MM-YYYY)	2. REPORT TYPE	3. DATES COVERED (From - To)
11-03-2014	Final Report	12-Aug-2013 - 12-Feb-2014

4. TITLE AND SUBTITLE
Application of Koopman Mode Decomposition Methods in Dynamic Stall

5a. CONTRACT NUMBER

5b. GRANT NUMBER
W911NF-13-C-0081

5c. PROGRAM ELEMENT NUMBER
611102

6. AUTHORS
Maria Fonoberova, Igor Mezic, Sophie Loire

5d. PROJECT NUMBER

5e. TASK NUMBER

5f. WORK UNIT NUMBER

7. PERFORMING ORGANIZATION NAMES AND ADDRESSES
AIMdyn, Inc
1919 State St, suite 207

Santa Barbara, CA 93101 -8455

8. PERFORMING ORGANIZATION REPORT NUMBER

9. SPONSORING/MONITORING AGENCY NAME(S) AND ADDRESS (ES)
U.S. Army Research Office
P.O. Box 12211
Research Triangle Park, NC 27709-2211

10. SPONSOR/MONITOR'S ACRONYM(S)
ARO

11. SPONSOR/MONITOR'S REPORT NUMBER(S)
64018-EG.1

12. DISTRIBUTION AVAILIBILITY STATEMENT
Approved for Public Release; Distribution Unlimited

13. SUPPLEMENTARY NOTES
The views, opinions and/or findings contained in this report are those of the author(s) and should not contrued as an official Department of the Army position, policy or decision, unless so designated by other documentation.

14. ABSTRACT
Dynamic stall is an inherently unsteady phenomenon which is significantly affected by the interaction of the laminar/turbulent boundary layer transition, flow separation, vortex growth and propagation, and reattachment of the flow. During dynamic stall, large peaks in lift, pitching moment and drag appear, and these cause an undesirable increase in the mean drag. Dynamic stall can also lead to potentially fatal structural loads due to strong vibrations of flexible aerodynamic surfaces. Despite extensive analytical, numerical, and experimental efforts to study dynamic stall motivated by the interest in improving maneuverability and performance of rotorcraft air vehicles

15. SUBJECT TERMS
Dynamic Stall, Koopman Mode Decomposition

16. SECURITY CLASSIFICATION OF:			17. LIMITATION OF ABSTRACT	15. NUMBER OF PAGES	19a. NAME OF RESPONSIBLE PERSON
a. REPORT	b. ABSTRACT	c. THIS PAGE			Maria Fonoberova
UU	UU	UU	UU		19b. TELEPHONE NUMBER 805-687-6999

Report Title

Application of Koopman Mode Decomposition Methods in Dynamic Stall

ABSTRACT

Dynamic stall is an inherently unsteady phenomenon which is significantly affected by the interaction of the laminar/turbulent boundary layer transition, flow separation, vortex growth and propagation, and reattachment of the flow. During dynamic stall, large peaks in lift, pitching moment and drag appear, and these cause an undesirable increase in the mean drag. Dynamic stall can also lead to potentially fatal structural loads due to strong vibrations of flexible aerodynamic surfaces. Despite extensive analytical, numerical, and experimental efforts to study dynamic stall motivated by the interest in improving maneuverability and performance of rotorcraft air vehicles, progress is needed for the full understanding and prediction of the relevant complex fluid dynamic mechanisms. Dominant mode extraction methods provide simplification of the unsteady flow phenomena by separating them into individual modes. Proper Orthogonal Decomposition of the velocity field is a popular technique to achieve this goal. However it can only reveal the energetically dominant coherent flow patterns, and has been shown to fail to capture subtle, oscillatory phenomena that are known to be important in dynamic stall physical processes such as the shear layer separation. We propose higher resolution models of dynamic stall.

Enter List of papers submitted or published that acknowledge ARO support from the start of the project to the date of this printing. List the papers, including journal references, in the following categories:

(a) Papers published in peer-reviewed journals (N/A for none)

Received Paper

TOTAL:

Number of Papers published in peer-reviewed journals:

(b) Papers published in non-peer-reviewed journals (N/A for none)

Received Paper

TOTAL:

Number of Papers published in non peer-reviewed journals:

(c) Presentations

Number of Presentations: 0.00

Non Peer-Reviewed Conference Proceeding publications (other than abstracts):

Received Paper

TOTAL:

Number of Non Peer-Reviewed Conference Proceeding publications (other than abstracts):

Peer-Reviewed Conference Proceeding publications (other than abstracts):

Received Paper

TOTAL:

Number of Peer-Reviewed Conference Proceeding publications (other than abstracts):

(d) Manuscripts

Received Paper

TOTAL:

Number of Manuscripts:

Books

Received Paper

TOTAL:

Patents Submitted

Patents Awarded

Awards

Graduate Students

NAME	PERCENT_SUPPORTED

FTE Equivalent:
Total Number:

Names of Post Doctorates

NAME	PERCENT_SUPPORTED

FTE Equivalent:
Total Number:

Names of Faculty Supported

NAME	PERCENT_SUPPORTED

FTE Equivalent:
Total Number:

Names of Under Graduate students supported

NAME	PERCENT_SUPPORTED

FTE Equivalent:
Total Number:

Student Metrics

This section only applies to graduating undergraduates supported by this agreement in this reporting period

The number of undergraduates funded by this agreement who graduated during this period: 0.00

The number of undergraduates funded by this agreement who graduated during this period with a degree in science, mathematics, engineering, or technology fields:..... 0.00

The number of undergraduates funded by your agreement who graduated during this period and will continue to pursue a graduate or Ph.D. degree in science, mathematics, engineering, or technology fields:..... 0.00

Number of graduating undergraduates who achieved a 3.5 GPA to 4.0 (4.0 max scale):..... 0.00

Number of graduating undergraduates funded by a DoD funded Center of Excellence grant for Education, Research and Engineering:..... 0.00

The number of undergraduates funded by your agreement who graduated during this period and intend to work for the Department of Defense 0.00

The number of undergraduates funded by your agreement who graduated during this period and will receive scholarships or fellowships for further studies in science, mathematics, engineering or technology fields:..... 0.00

Names of Personnel receiving masters degrees

NAME
Total Number:

Names of personnel receiving PHDs

NAME
Total Number:

Names of other research staff

NAME	PERCENT_SUPPORTED
Maria Fonoberova	0.70
Igor Mezic	0.10
Sophie Loire	0.30
FTE Equivalent:	**1.10**
Total Number:	**3**

Sub Contractors (DD882)

Inventions (DD882)

Scientific Progress

See Attachment

Technology Transfer

Project Title: Application of Koopman Mode Decomposition Methods in Dynamic Stall
Contract Number: W911NF-13-C-0081
Proposal Number: 64018EG
Period: August 12, 2013 – February 11, 2014
PI: Dr. Maria Fonoberova
Institution: AIMdyn, Inc.

Final Technical Report

Introduction

There is currently much interest in the unsteady aerodynamics of flows relevant to rotorcraft (manned and unmanned) air vehicles. The flow fields in these applications exhibit unsteady separation followed by the formation of dynamic-stall-like vortices whose evolution and interaction with flexible aerodynamic surfaces have a significant impact on flight stability and performance. Analysis of these flows is complicated further by their mixed laminar transitional turbulent character at moderate Reynolds numbers, as well as by the broad range of possible parameters, kinematics, and configurations. To facilitate progress in the understanding and prediction of the relevant fluid dynamic mechanisms, it is natural to consider methods that provide simplification of the flow phenomena by separating them into individual modes. The technique of Proper Orthogonal Decomposition (POD) is a popular way of accomplishing this task. However, while POD is capable of extracting the most energetic parts of the flow field, it has been shown to lack ability of highlighting subtle, oscillatory phenomena that are nevertheless implicated in important physical processes such as the shear layer separation.

Unsteady flows over plunging and pitching airfoils with large excursions in effective angle of attack exhibit the phenomenon termed dynamic stall, a process characterized by unsteady separation and by the formation of large-scale leading-edge and trailing-edge vortices, which exert difficult-to-predict variations in aerodynamic loads. Comprehensive reviews of this phenomenon, first discovered and studied extensively in the context of helicopter rotor blades, has been given in [1,3,8].

The initial research has suggested existence of high-frequency effects in leading edge vortex shedding events, not present in the static stall case. The purpose of the project was to advance this approach using Aimdyn's development of Koopman operator mode decomposition techniques.

Computation of Koopman Modes

Koopman mode decomposition is based on the surprising fact, discovered in [5], that normal modes of linear oscillations have its natural analogue - Koopman modes - in the context of nonlinear dynamics. To pursue this analogy, one must change the representation of the system from the state-space representation to the dynamics governed by the linear Koopman operator ([4]) on an infinite-dimensional space of observables. Contrary to the proper orthogonal decomposition, the dynamic mode decomposition contains not only information about coherent structures, but also about their temporal evolution.

Based on snapshots of the flow, we can approximate the Koopman Modes using an Arnoldi-like algorithm sometimes called dynamic mode decomposition (DMD) ([9,10]) which computes eigenvalues based on the so-called companion matrix.

Given a sequence of equispaced in time snapshots from numerical simulations or physical experiments, with Δt being the time interval between snapshots, a data matrix is formed with columns that represent the individual data samples $u_j \in R^n, j = 0, \dots, m$, with j representing time $j\Delta t$. The companion matrix is then defined as:

$$C = \begin{pmatrix} 0 & 0 & \cdots & 0 & c_0 \\ 1 & 0 & & 0 & c_1 \\ 0 & 1 & & 0 & c_2 \\ \vdots & & \ddots & & \vdots \\ 0 & 0 & \cdots & 1 & c_{m-1} \end{pmatrix}$$

where $c_i, i = 0, \dots, m-1$ are such that:

$$u_m = \sum_{j=0}^{m-1} c_i u_i + r$$

and r is the residual vector.

The spectrum of the Koopman operator restricted to the subspace spanned by u_j is equal to the spectrum of the infinite-dimensional companion matrix and the associated Koopman modes are given by Ka (provided that a does not belong to the null space of K), where $K = [u_0, u_1, \dots, u_{m-1}]$ is the column matrix (vector-valued) of observables snapshots at times $0, \Delta t, \dots, (m-1)\Delta t$ and a is an eigenvector of the shift operator restricted to Krylov subspace spanned by u_i which the Companion matrix is an approximation of. The approximate Koopman eigenvalues and eigenvectors obtained by the Arnoldi's algorithm are called Ritz eigenvalues and eigenvectors.

The standard Arnoldi-type algorithm to calculate the Ritz eigenvalues λ_j and eigenfunctions v_j is as follows:

1. Define $K = [u_0, u_1, \dots, u_{m-1}]$.

2. Find constants c_j such that:

$$r = u_m - \sum_{j=0}^{m-1} c_j u_j = u_m - Kc,\ r \perp span\{u_0, ..., u_{m-1}\}.$$

This can be done by defining $c = K^+ u_m$, where K^+ is the pseudo inverse of K.

3. Define the companion matrix C as above and find its eigenvalues and eigenvectors:

$$C = T^{-1}\Lambda T, \Lambda = diag(\lambda_1, \cdots, \lambda_m),$$

where eigenvectors are columns of T^{-1}. Note that the Vandermonde matrix $\tilde{T}$

$$\tilde{T} = \begin{pmatrix} 1 & \lambda_1 & \lambda_1^2 & \cdots & \lambda_1^{m-1} \\ 1 & \lambda_2 & \lambda_2^2 & \cdots & \lambda_2^{m-1} \\ \vdots & \vdots & \vdots & \ddots & \vdots \\ 1 & \lambda_m & \lambda_m^2 & \cdots & \lambda_m^{m-1} \end{pmatrix}$$

diagonalizes the companion matrix C , as long as the eigenvalues $\lambda_1, \ldots, \lambda_m$ are distinct.

4. Define v_j to be the columns of $V = K\tilde{T}^{-1}$.

Then, the Arnoldi-type Koopman Mode Decomposition gives:

$$\forall k = [0, 1, \cdots, m],\ u_k = \sum_{j=1}^{m} \lambda_j^k V(:, j)$$

In order for the result of an Arnoldi-type method to give a good approximation of the Koopman modes, the companion matrix C should be a good matrix representation of the projection of the Koopman operator on a Krylov subspace. The algorithm described above uses a least-square approximation. However, the known properties of the Koopman operator are ignored in the above algorithm:

- ✓ Constant functions are eigenfunctions of the Koopman operator at eigenvalue 1. Hence the Companion matrix as an approximation of the Koopman operator should have an eigenvalue at 1. This condition can be translated as: $\sum_{j=0}^{m-1} c_j = 1$.

- ✓ When the signal is periodic on the attractor such that $u_0 = u_m$, the DMD computation should reduce to Discrete Fourier Transform [2]. In that case, the companion matrix coefficient should be $c_0 = 1, c_j = 0, \forall j > 0$ and the algorithm computing the Koopman Modes should be able to approximate those values of c_j automatically.

A new Arnoldi-type algorithm has been developed at Aimdyn. It is similar to the standard one but includes the known properties described above by replacing step 2 of the algorithm where the constants c_j are computed by:

$$c = \tilde{K}^+ \tilde{u}_m,$$

where

$$\tilde{K} = \begin{pmatrix} u_1 & u_2 & \cdots & u_{m-1} \\ 1 & 1 & \cdots & 1 \end{pmatrix}, \tilde{u}_m = \begin{pmatrix} u_m - u_0 \\ 0 \end{pmatrix}$$

and $\tilde{K}^+$ is the pseudo inverse of $\tilde{K}$.

Analysis of a 2D simulation data for 1 period of airfoil oscillation

By using the described above techniques a simulation data set from Dr. Miguel Visbal at the AFRL was analyzed. The files were 360 snapshots of 2D grid and flow data for 1 period of airfoil oscillation. The flow was spanwise-averaged so that small scales structures are reduced. The obtained data was processed for plotting (see Figure 1 that shows u horizontal velocity, v vertical velocity, w out of plane velocity, p pressure and rho density at phase $\pi/2$).

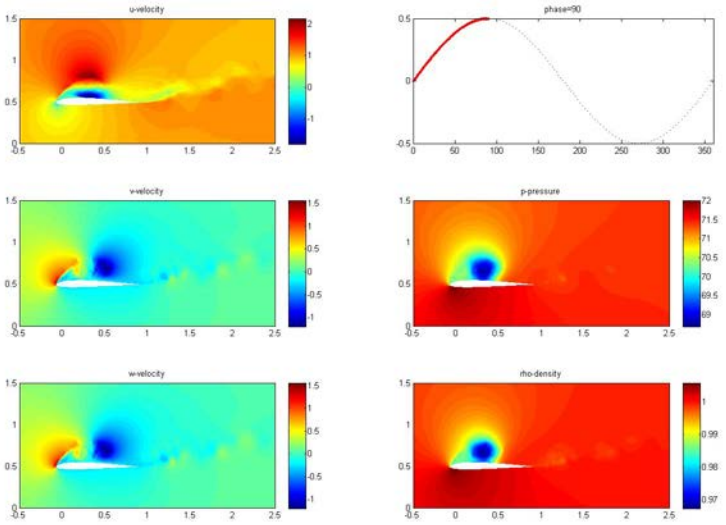

Figure 1. Dynamic Stall of a Plunging Airfoil 2D simulation data sets at phase $\pi/2$ of the plunging motion, u horizontal velocity, v vertical velocity, w out of plane velocity, p pressure and rho density.

Due to the large size of the data set, using Matlab for data processing reaches its limit. AIMdyn's team implemented the Koopman Mode Decomposition algorithm in C++ to be able to process very large sets of data.

A new, Arnoldi-type method developed by Aimdyn was used for Koopman Mode Decomposition. Figure 2 shows Fourier and KMD spectrum for u-velocity.

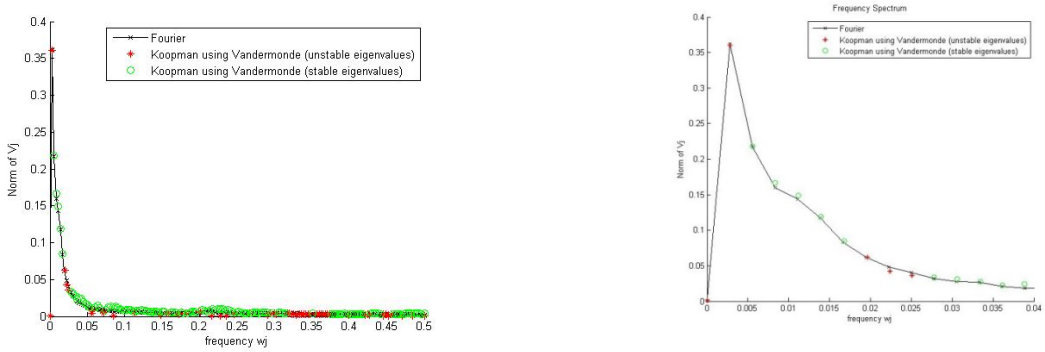

Figure 2. Fourier and KMD spectrum for u-velocity. (left) Frequencies from 0 to 0.5. (right) Close-up for frequencies from 0 to 0.04. The amplitude is calculated as the norm of all amplitudes over all spatial points. FFT is in black; unstable KM spectrum is red; stable KM spectrum is green.

The obtained Koopman mode eigenvalues are shown in Figure 3.

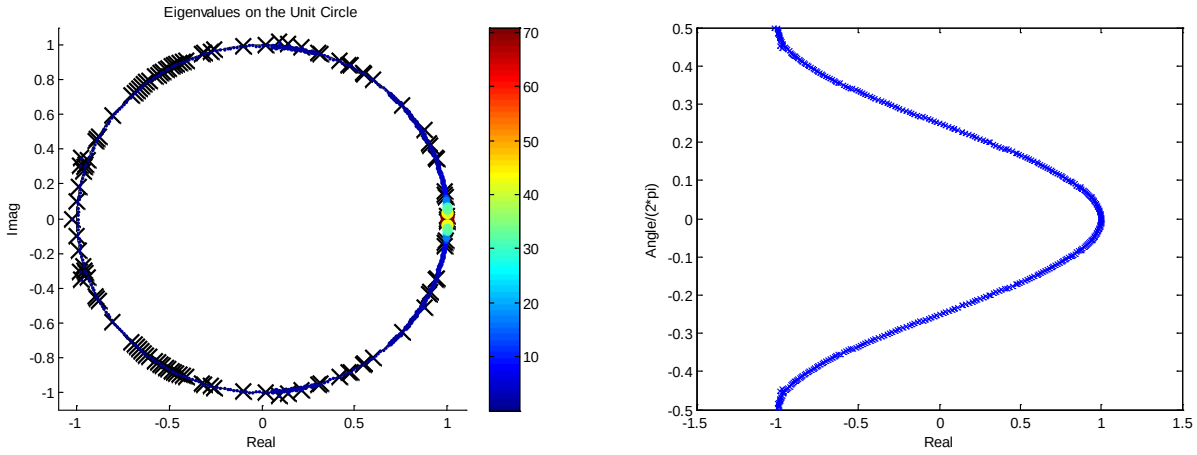

Figure 3. Koopman Mode Eigenvalues.

Fourier and KMD spectrum for several regions of interest for u velocity (see Figure 4) are shown in Figure 5.

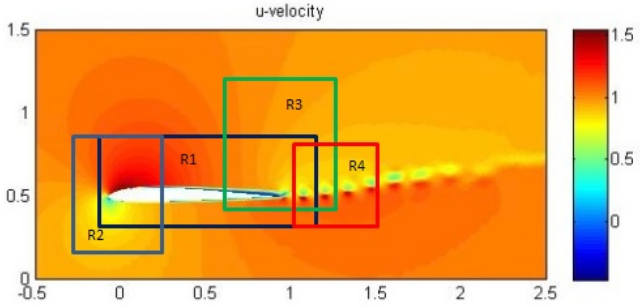

Figure 4. Regions of interest for u velocity.

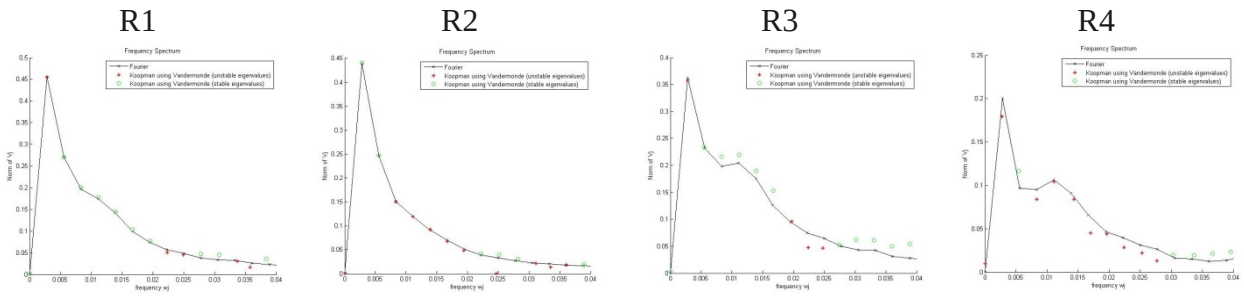

Figure 5. Fourier and KMD spectrum for four regions of interest for u-velocity. FFT is in black; unstable KM spectrum is red; stable KM spectrum is green.

The frequency spectrum and the magnitude of modes corresponding to frequency 0.027 Hz and frequency 0.011 Hz for the u-velocity probe with coordinates (1.04; 0.50) are shown in Figure 6.

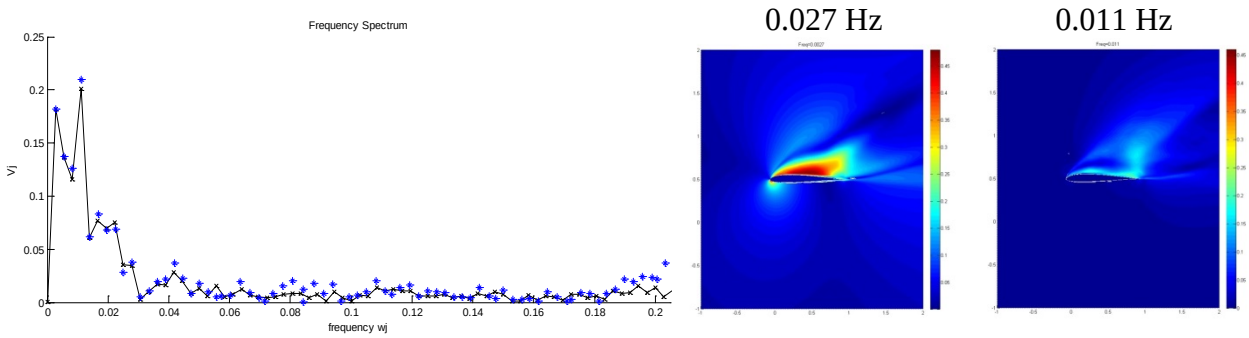

Figure 6. Fourier and KMD spectrum for a point of u-velocity with (1.04; 0.50) coordinates. FFT is in black; KM spectrum is blue. Magnitude for the Koopman mode corresponding to frequency 0.027 Hz and frequency 0.011 Hz.

Using Koopman mode decomposition technique processing of a 2D data set the team members studied details of the physics of dynamic stall.

Similarity of the Koopman mode decomposition of the dynamic stall and the cylinder wake with oscillating Re number forcing

We developed a model system that is capable of revealing physics of the dynamic stall in a simpler setting. The model system is a cylinder in an incoming oscillatory flow. It provided us with some remarkable insight. In the following we describe the simulation and some results.

The cylinder wake simulation was provided by Dr. Bryan Glaz at the U.S. Army Research Laboratory. The cylinder was 0.002m in diameter. Flow snapshots were outputted starting at the 25th time step, up to the 60,000th time step in increments of 25 time steps (each time step is 1e-4 s). The total time length corresponds to 12 periods of the driving frequency, which is 2Hz. The number of nodes in the grid is 29954.

From 0.0s to 0.5s (i.e. 5000 iterations) Reynolds number (Re) was 58.3 that corresponds to incoming velocity of 0.5 m/s. The critical Re for a cylinder is about Re~40 when it starts exhibiting the von Karman wake instability. So the interval from 0 to 0.5 s at Re=58.3 corresponds to the Landau equation when the external input is greater than the bifurcation value. Then, starting at 0.5 seconds, the Re is being oscillated by oscillating incoming velocity. The oscillating Re corresponded to Re = 58.3 + 35*sin(2pi*omega*t), where omega corresponded to 2 Hz. The reason 35 was selected for the oscillating Re amplitude is because a large enough amplitude was needed such that the Re would oscillate above and below the critical value predicted by the regular Landau equation. The reason 2 Hz was selected is that it's an order of magnitude slower than the von Karman vortex frequency, which is about 39 Hz for Re = 58.3. It was planned so that the driving frequency to be about an order of magnitude lower than the flow instability frequency because the dynamic stall driving frequency is about 1-2 orders of magnitude slower than the shear layer, wake dynamics for the airfoil. So the goal was to setup a cylinder problem where there is a significant separation in time scales.

The Koopman spectrum plots are shown in Figure 7. It is remarkable how the spectrum shown at the bottom becomes broad upon introduction of the low-frequency oscillation, in contrast to the clean peak at 40 for the von Karman vortex flow in the top of that figure. An analytical understanding of that is lacking, despite a number of dynamical system bifurcation studies (e.g. [7]) and we plan to investigate it in the future work.

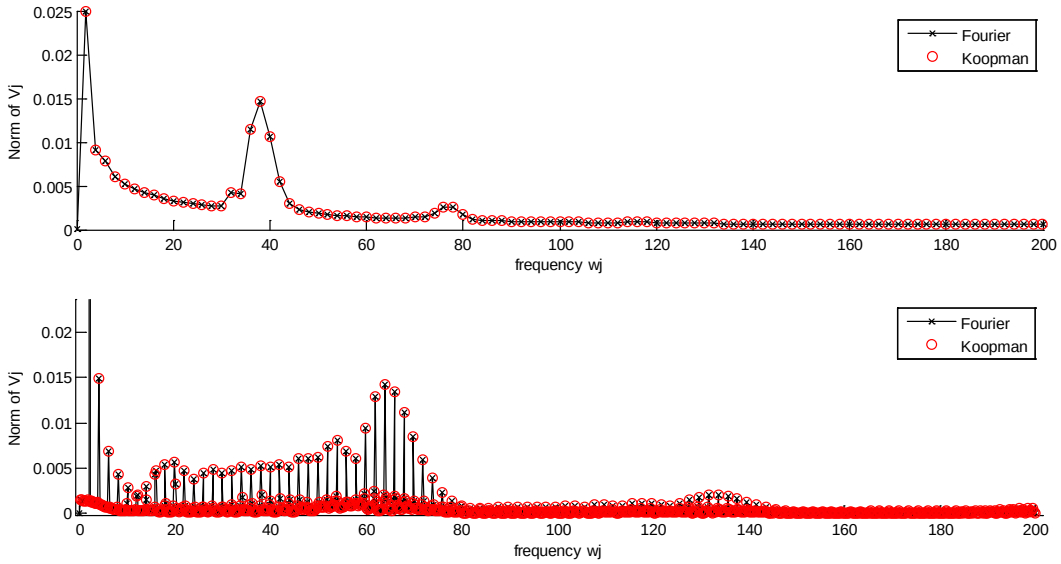

Figure 7. Spectrum of von Karman vortex shedding flow around a cylinder (top) and the flow around the same cylinder when the incoming velocity is oscillated (bottom). Note the broadening of the spectrum, similar to the pitching wing spectrum, and the high frequency component around 120.

The interesting spectrum-broadening effect for flow around cylinder in incoming flow of oscillating magnitude leads us to believe that further investigation of this model might shed physical insight on the wing pitching and plunging model, that also has broad spectrum.

In [2], the observation is made that subtracting the mean of the sequence of snapshots leads to the result of all possible eigenvalues being on the unit circle, the companion matrix analysis reducing essentially to the Discrete Fourier Transform, however in [6], it is shown that this is true for finite m only if the observable snapshots are periodic with $u_0 = u_m$.

For the described above cylinder wake simulation the Koopman Mode Decomposition (by using Arnoldi-type algorithm) was performed for:
case A: subtracting the mean of the sequence of snapshots;
case B: without subtracting the mean of the sequence of snapshots.

Case B was studied for the two following sub-cases:
case B1: not-normalizing each column of the inverse to the Vandermonde matrix $\tilde{T}^{-1}$;
case B2: normalizing each column of the inverse to the Vandermonde matrix $\tilde{T}^{-1}$.

Note that in the case of subtracting the mean, the normalized and not-normalized cases are very similar.

Figure 8 shows Fourier and KMD spectrum for u-velocity for the whole simulation time for cases A, B1 and B2.

case A

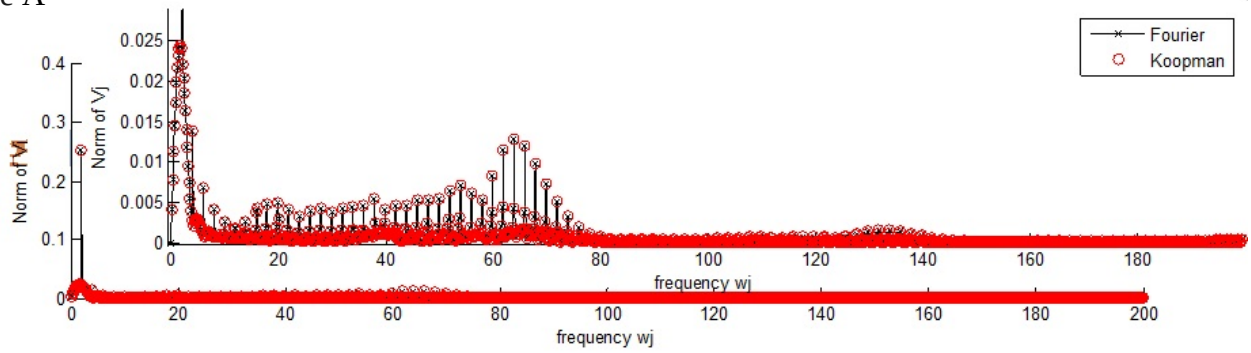

case B1

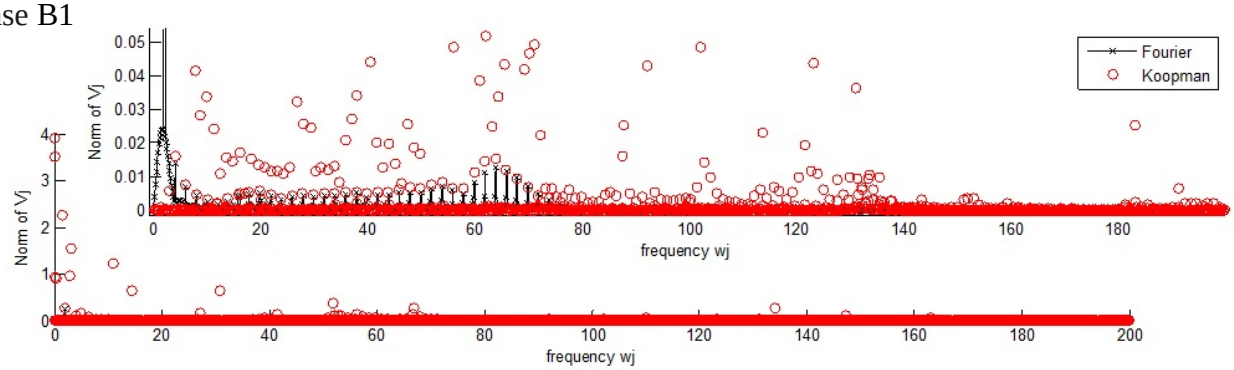

case B2

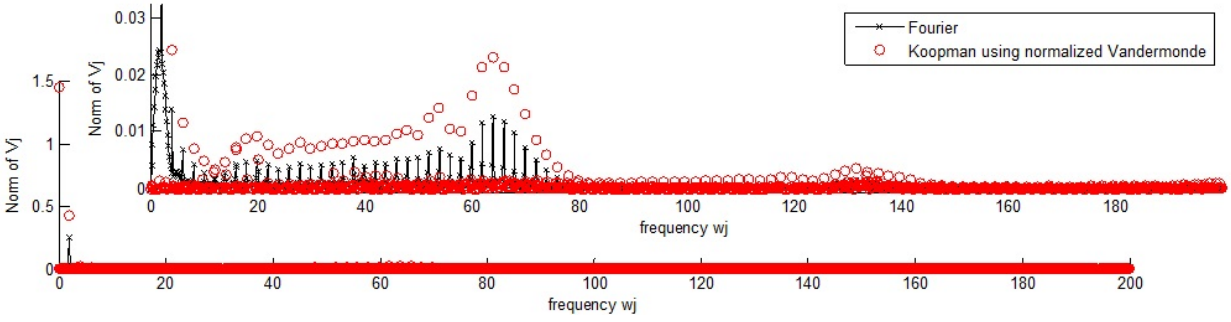

Figure 8. Fourier and KMD spectrum for u-velocity for the whole simulation time. FFT is in black; KM spectrum is red.

The obtained Koopman mode eigenvalues are shown in Figure 9.

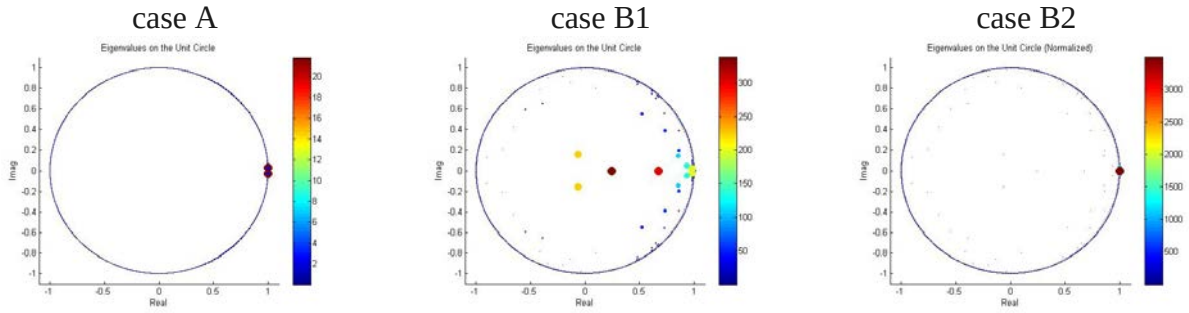

Figure 9. Koopman Mode Eigenvalues for u-velocity for the whole simulation time.

Figure 10 shows the DMD spectrum in frequency w, exponential rate mu plane.

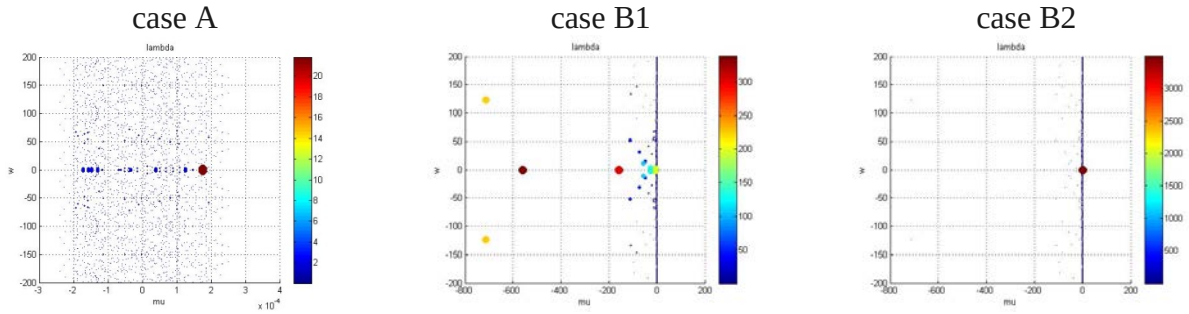

Figure 10. DMD spectrum in frequency w, exponential rate mu plane for u-velocity for the whole simulation time.

Magnitude, phase, real part and imaginary part for the Koopman modes corresponding to frequency 2 and 63.83 Hz for case A are shown in Figure 11.

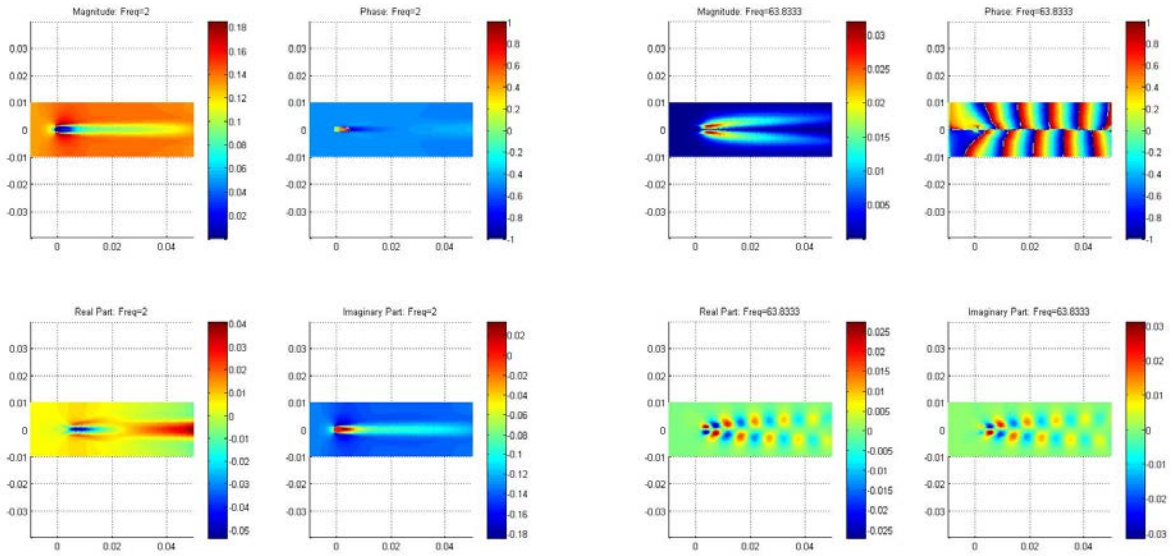

Figure 11. Magnitude, phase, real part and imaginary part for the Koopman mode for u-velocity for the whole simulation time for case A corresponding to frequency 2 Hz (left) and 63.83 Hz (right).

The recomposition of signal using 20 pairs of the highest magnitude modes sorted by abs of norm of Vj has been performed. Figure 12 shows the reconstructed signal (red) vs the original data (blue) for the random location and the dependence of the mean of the recomposition error (L2 norm of the difference between signal and recomposed signal divided by the L2 norm of the signal) on the number of modes used.

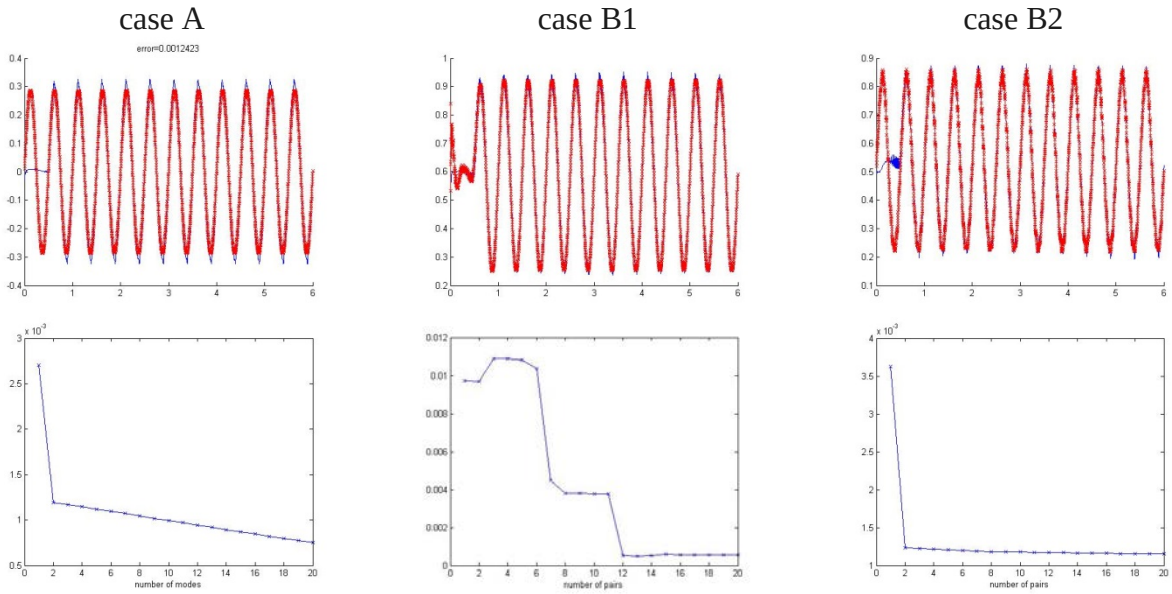

Figure 12. (Top) The reconstructed signal (red) vs the original data (blue) for a random location, (Bottom) the dependence of the mean of the recomposition error (L2 norm of the difference between signal and recomposed signal divided by the L2 norm of the signal) on the number of modes used for u velocity for the whole simulation time.

Figure 13 shows the histogram of the recomposition error over all locations if using only 4 modes (frequencies 2 Hz, -2 Hz, 63.83 Hz and -63.83 Hz) and the recomposition of signal that gives the median error for case A.

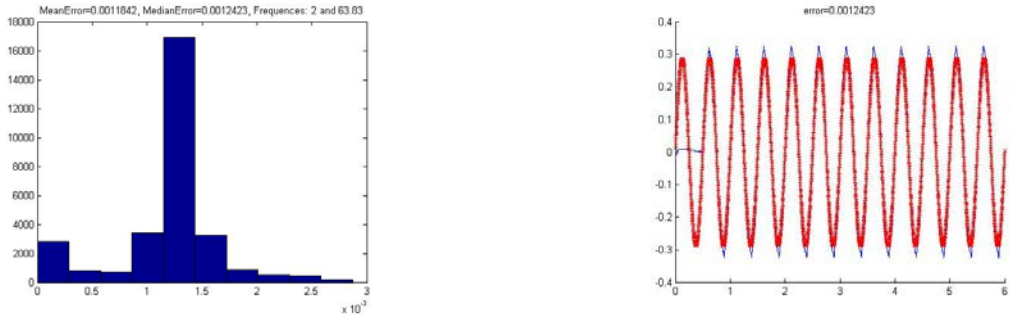

Figure 13. (Left) The histogram of the recomposition error over all locations if using only 4 modes (frequency 2, -2, 63.83 and -63.83), (Right) the recomposition of signal (red – reconstructed signal, blue – data) that gives the median error for u velocity for the whole simulation time for case A.

Figure 14 shows Fourier and KMD spectrum for u-velocity for the first period of the simulation time after removing first 500 iterations for cases A, B1 and B2.

case A

case B1

case B2

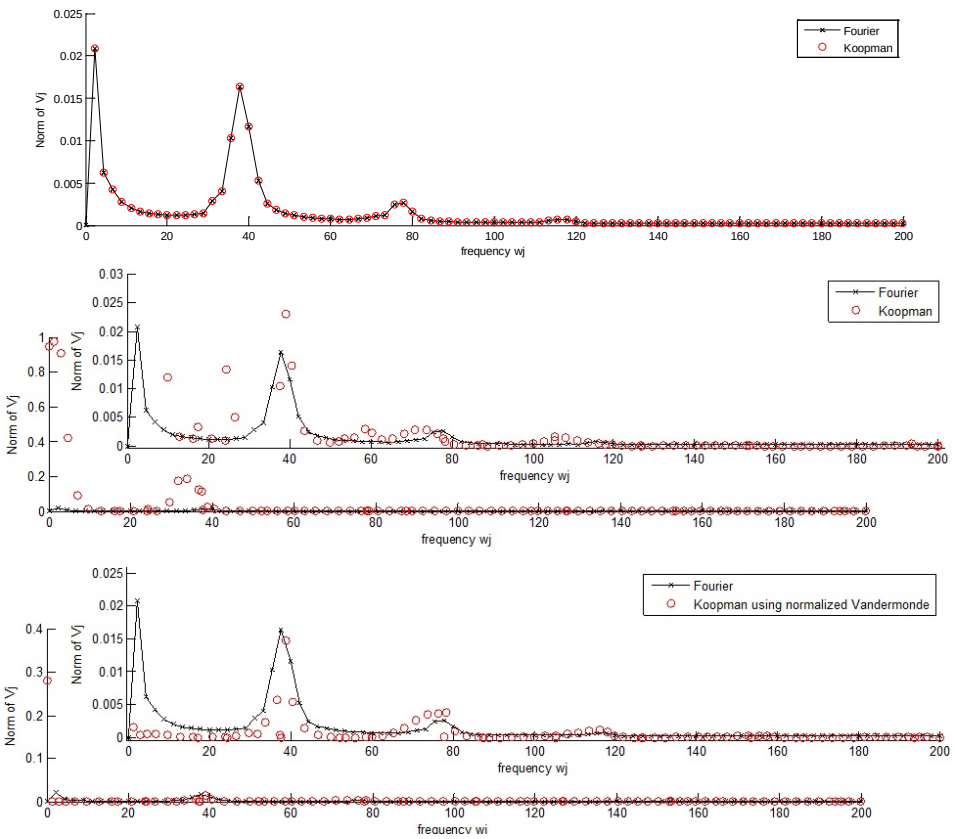

Figure 14. Fourier and KMD spectrum for u-velocity for the first period of the simulation time. FFT is in black; KM spectrum is red.

The obtained Koopman mode eigenvalues are shown in Figure 15.

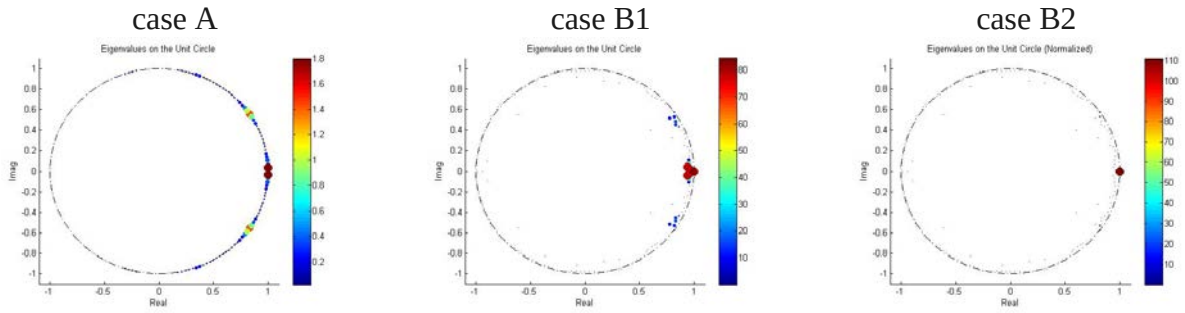

Figure 15. Koopman Mode Eigenvalues for u-velocity for the first period of the simulation time.

Figure 16 shows the DMD spectrum in frequency w, exponential rate mu plane.

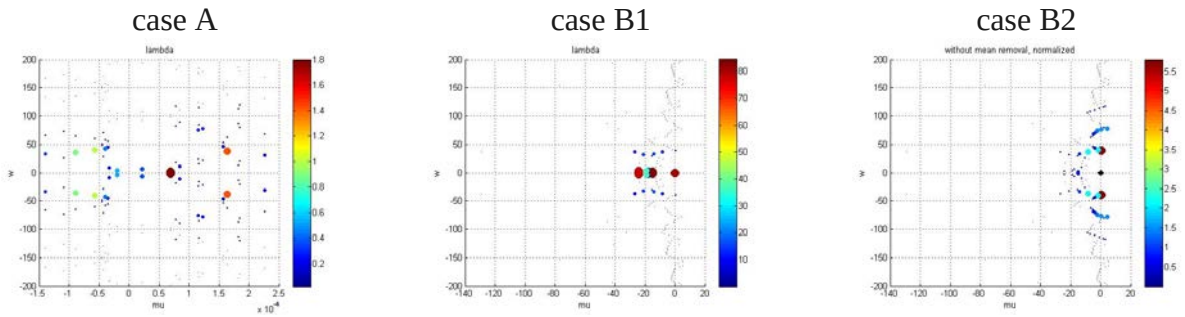

Figure 16. DMD spectrum in frequency w, exponential rate mu plane for u-velocity for the first period of the simulation time.

Magnitude, phase, real part and imaginary part for the Koopman modes for case A corresponding to frequency 2 Hz and 38 Hz are shown in Figure 17.

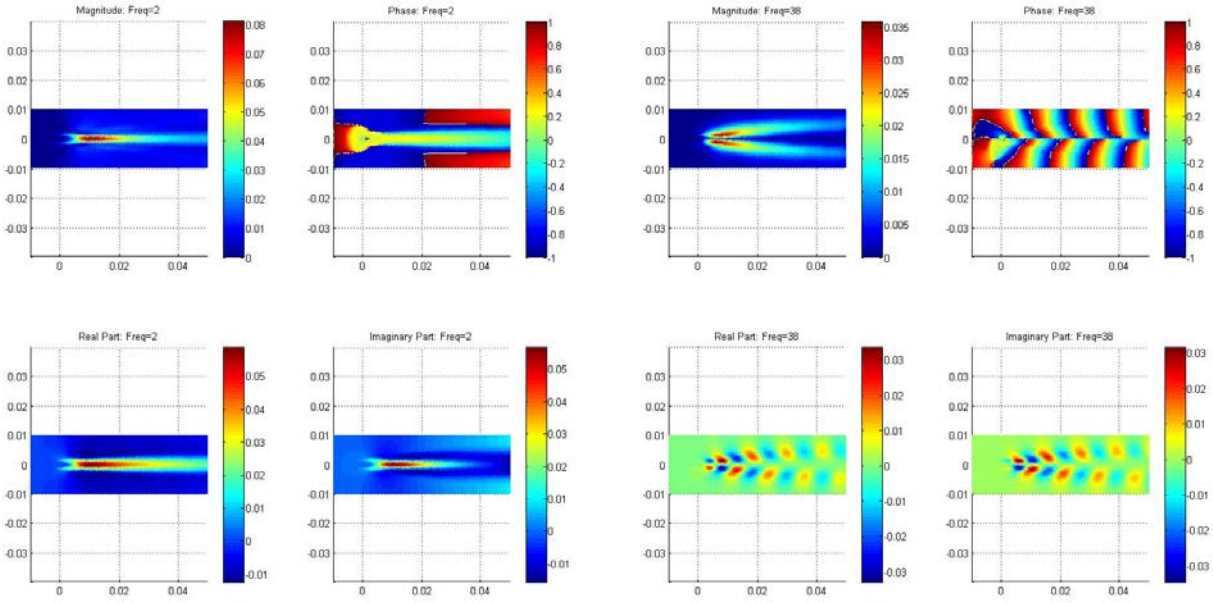

Figure 17. Magnitude, phase, real part and imaginary part for the Koopman mode for u-velocity for the first period of the simulation time for case A corresponding to frequency 2 Hz (left) and 38 Hz (right).

The recomposition of signal using 20 pairs of the highest magnitude modes sorted by abs of norm of Vj has been performed. Figure 18 shows the reconstructed signal (red) vs the original data (blue) for the random location.

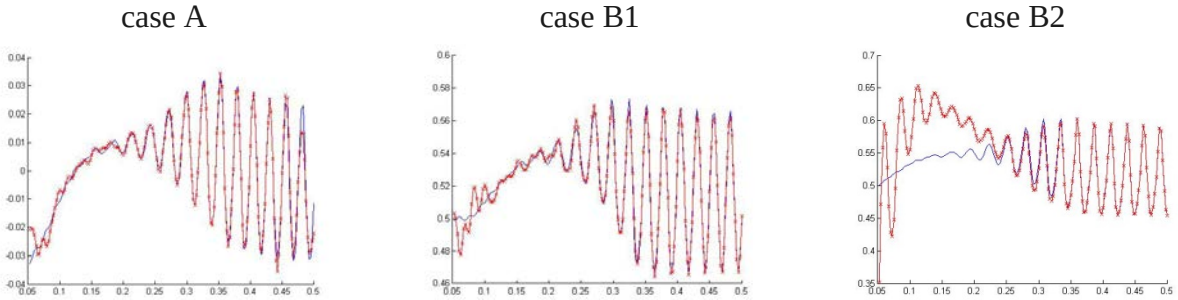

Figure 18. The reconstructed signal (red) vs the original data (blue) for a random location for u velocity for the first period of the simulation time.

The Koopman Mode Decomposition of the model system that we have pursued shows remarkable ability to reconstruct signal coming from such a broad-spectrum flow.

Conclusions

The initial analysis of dynamic stall using the methods of Koopman operator theory was performed. This research guided by dynamical systems methods and efficient numerical methods for Koopman Mode Decomposition lead to some interesting outcomes. Among those are insight into the physical effects of the oscillatory nature of the incoming velocity that the wing experiences due to pitch or plunging. For example, the examination of a model system - a cylinder in an incoming oscillatory flow - showed some of the physical effects (e.g. broadening of the spectrum) observed in the pitching airfoil case are present in the model system and shed light on the dynamics of aspects of pitching airfoil dynamics as a nonlinear interaction of the forcing by the oscillating incoming flow frequency and natural frequency of vortex shedding dynamics.

References

[1] L.W. Carr. Progress in analysis and prediction of dynamic stall. Journal of Aircraft, 25(1), 1987.
[2] K. Chen, J. Tu, and C. Rowley. Variants of dynamic mode decomposition: Boundary condition, koopman, and fourier analyses. Journal of Nonlinear Science, 887-915, 2012.
[3] J.A. Ekaterinaris and M.F. Platzer. Computational prediction of airfoil dynamic stall. Progress in aerospace sciences, 33(11-12):759-846, 1998.
[4] B.O. Koopman. Hamiltonian systems and transformation in Hilbert space. Proceedings of the National Academy of Sciences of the United States of America, 17(5):315, 1931.
[5] I. Mezic. Spectral properties of dynamical systems, model reduction and decompositions. Nonlinear Dynamics, 41(1):309-325, 2005.
[6] I. Mezic. Analysis of fluid flows via spectral properties of koopman operator. Annual Review of Fluid Mechanics, Vol. 45: 357-378, 2013
[7] R Mettin, U Parlitz, and W Lauterborn. Bifurcation structure of the driven van der pol oscillator. International Journal of Bifurcation and Chaos, 3(06):1529{1555, 1993.
[8] WJ McCroskey. Unsteady airfoils. Annual Review of Fluid Mechanics, 14(1):285-311, 1982.
[9] P. Schmid and J. Sesterhenn. Dynamic mode decomposition of numerical and experimental data. 61st Annual Meeting of the APS Division of Fluid Dynamics, November 2008.
[10] C.W. Rowley, I. Mezic, S. Bagheri, P. Schlatter, and D.S. Henningson. Spectral analysis of nonlinear flows. Journal of Fluid Mechanics, 641(1):115-127, 2009.